

# REPORT DOCUMENTATION PAGE

Form Approved  
OMB No. 0704-0188

Public reporting burden for 2014 collection of information is estimated to average 1 "hour per report" including the time for reviewing instructions, searching existing data sources, gathering and maintaining the data needed, and completing and reviewing the collection of information. Send comments regarding this burden estimate or any other aspect of this collection of information, including suggestions for reducing this burden, to Washington Headquarters Services, Directorate for Information Operations and Reports, 1215 Jefferson Davis Highway, Suite 1204, Arlington, VA 22202-4302, and to the Office of Management and Budget: Paperwork Reduction Project (0704-0188) Washington, DC 20503.

<b>1. AGENCY USE ONLY (Leave Blank)</b>			<b>2. REPORT DATE</b> 1 Jul 97	<b>3. REPORT TYPE AND DATES COVERED</b> Progress Report 1 Apr 97 - 30 Jun 97
<b>4. TITLE AND SUBTITLE</b>  <del>Synthesis and Processing of Nanocrystalline Titanium Nitride</del>			<b>5. FUNDING NUMBERS</b> G - N00014-95-1-0626	
<b>6. AUTHOR(S)</b> Jackie Y. Ying				
<b>7. PERFORMING ORGANIZATION NAME(S) AND ADDRESS(ES)</b>  Department of Chemical Engineering Massachusetts Institute of Technology 77 Massachusetts Avenue, Room 66-544 Cambridge, MA 02139-4307			<b>8. PERFORMING ORGANIZATION REPORT NUMBER</b>	
<b>9. SPONSORING/MONITORING AGENCY NAME(S) AND ADDRESS(ES)</b>  Office of Naval Research 800 North Quincy Street Ballston Tower One Arlington, VA 22217-5660			<b>10. SPONSORING/MONITORING AGENCY REPORT NUMBER</b>	
<b>11. SUPPLEMENTARY NOTES</b>				
<b>12a. DISTRIBUTION/AVAILABILITY STATEMENT</b>  Approved for public release; distribution unlimited.			<b>12b. DISTRIBUTION CODE</b>	
<b>13. ABSTRACT (Maximum 200 words)</b>  <p>With careful powder handling procedures and processing, the nanocrystalline TiN produced in our novel reactor undergoes tremendous sintering and densification to produce dense (99%) TiN materials at 1400 °C in a simple, pressureless sintering process. This report outlines the determination of mechanical properties of these materials and contains a benchmark comparison of these properties, and the processing required to achieve them, against other TiN materials reported in the literature. The nanostructured TiN materials processed via the pressureless sintering process had a <math>H_v</math> hardness value of <math>23.2 \pm 1.9</math> GPa, among the highest recorded in the literature for TiN, and a <math>K_c</math> fracture toughness of <math>4.0 \pm 0.2</math> MPa<math>\text{m}^{1/2}</math>. These sintering and property results are particularly noteworthy in comparison to those noted previously in the literature due to the complicated processing conditions required by other researchers utilizing lower quality starting powders.</p>				
<b>14. SUBJECT TERMS</b> Nanocrystalline Processing, Titanium Nitride			<b>15. NUMBER OF PAGES</b> 6	
<b>16. PRICE CODE</b>				
<b>17. SECURITY CLASSIFICATION OF REPORT</b> UNCLASSIFIED	<b>18. SECURITY CLASSIFICATION OF THIS PAGE</b> UNCLASSIFIED	<b>19. SECURITY CLASSIFICATION OF ABSTRACT</b> UNCLASSIFIED	<b>20. LIMITATION OF ABSTRACT</b> UL	

"Nanocrystalline Processing and Interface Engineering of Si<sub>3</sub>N<sub>4</sub>-based Nanocomposites"

Technical Report on ONR Grant No. N00014-95-1-0626  
for the period of April 1, 1997 - June 30, 1997

Jackie Y. Ying  
St. Laurent Associate Professor  
Department of Chemical Engineering  
Massachusetts Institute of Technology  
Room 66-544, 77 Massachusetts Avenue  
Cambridge, MA 02139-4307  
Tel: (617) 253-2899  
FAX: (617) 253-3122

***Nanocrystalline TiN Processing and Properties***

With careful powder handling procedures and processing, the nanocrystalline TiN powders produced in our novel reactor undergo tremendous sintering and densification to produce dense (99%) TiN materials at 1400 °C in a simple, pressureless sintering process [1]. This quarter's efforts continued our work on the evaluation of these nanostructured TiN materials in two main areas [2]. The first area was the determination of mechanical properties of these materials, while the second focus was on benchmarking these properties, and the processing required to achieve them, against other TiN materials reported in the literature.

Data on hardness and fracture toughness was collected via Vickers hardness testing (LECO DM400). Testing was conducted on polished samples at 20 °C with loads of 0.5 – 3 N and deformation times of 15 seconds. Data represent averaged values for 10-15 indentations. The fracture toughness was also assessed via microhardness indentation testing. From the idea that the size of indentation cracks can be used to quantify toughness, Eqn. 1 was developed [3]:

$$K_c = 0.016 \pm 0.004 \left( \frac{E}{H} \right)^{\frac{1}{2}} \left( \frac{P}{c_o^{3/2}} \right) \quad (1)$$

where  $K_c$  is the fracture toughness,  $E$  is Young's modulus,  $H$  is the hardness as determined during the Vickers hardness test,  $P$  is the peak load during the test and  $c_o$  is the radial crack dimension. A literature value for  $E$  in TiN of 470 MPa was used for these experiments [4]. The nanostructured TiN materials processed via the pressureless sintering process described in previous reports [1] had a  $H_v$  hardness value of  $23.2 \pm 1.9$  GPa and a  $K_c$  fracture toughness of  $4.0 \pm 0.2$  MPa m<sup>1/2</sup>.

In order to facilitate comparison of the processing and property results in our TiN materials, Table 1 was prepared. Materials in that table are ranked by decreasing hardness. Because of different processing and measurement techniques, it should be noted that for all the hardness and grain size comparisons shown in the table, small differences in values are likely not significant. However, at the same time, it should be noted that our  $H_v$  result is among the very highest values reported for this parameter in TiN and is certainly higher than that observed in the conventionally sintered or hot-pressed conventional materials. Additionally, these hardness values were achieved in a pressureless sintering process without the use of applied pressure or sintering additives.

The values of  $H_v$  in Table 1 for TiN materials which are near full density and don't have some other interfering issue such as the 11.8 at% metals in Ogino's materials [16], can be plotted versus the inverse square root of grain size as shown in Figure 1. The data point for our nano-TiN materials is shown

19970707 052

as an oval in Figure 1. This plot indicates that TiN shows an increasing hardness ( $H$ ) with decreasing grain size ( $G$ ) as described by:

$$H = H_o + k G^{-1/2} \quad (2)$$

Down to a certain grain size this effect is observed for a majority of nanocrystalline metals and intermetallic compounds [18-20], but demonstrated instances of this behavior in nanocrystalline nitride ceramics are rare due to the difficulty in maintaining a fine grain size in a fully dense material. This same behavior has also been noted in nanocrystalline  $TiO_2$  [21]. Additionally, Averback *et al.* found for  $TiO_2$ , as we did for TiN, that the  $H_v$  of their dense nanocrystalline ceramic was about equal to that in the single crystal of the same material [21].

The effect of grain size on fracture strength, and thus hardness, in ceramics has generally been interpreted in terms of a dependence

$$\sigma = f(G^{-1/2}) \quad (3)$$

where  $\sigma$  is the fracture strength and  $G$  the grain size [22,23]. Davidge and Evans suggest that the strength of a ceramic may be controlled by either the stress to propagate inherent flaws or the stress to nucleate and/or propagate flaws formed during a plastic deformation process [22]. Thus, there are two regions for the variation of fracture strength with grain size, both of which show a  $G^{-1/2}$  dependence. At larger grain sizes, fracture is initiated at inherent flaws with a dependence

$$\sigma \propto \frac{1}{C^{1/2}} \quad (4)$$

where  $C$  is the inherent flaw or crack length [22]. This flaw size  $C$  is related to microstructural features such as the pore or grain size. In fact, it has been shown in fully dense  $MgO$  that  $C \propto G^{0.8}$  [22]; thus, in this first region (Region I), fracture occurs by the extension of inherent flaws and  $\sigma \propto G^{-1/2}$ . At finer grain sizes, dislocations may pile up against a stable barrier, such as a grain boundary, and a large stress concentration is generated in the vicinity of these dislocations. If this stress is not relieved by plastic flow, cracks may be initiated at the pile-up. The shear stress  $\tau$  is given by

$$\tau = \tau_o + \frac{k_s}{L^{1/2}} \quad (5)$$

where  $\tau_o$  is the dislocation flow stress,  $k_s$  is a term that depends on the effective surface energy for localized crack initiation and  $L$  is the length of the pile-up [22]. In this second region (Region II), with the grain boundary acting as a dislocation source, the minimum value for the crack initiation stress is obtained with  $L = G$ . Thus, in Region II at finer grain sizes, where fracture is initiated by plastic flow, again,  $\sigma \propto G^{-1/2}$ . Carniglia [23] has shown that strength/grain size data for various ceramics, including  $Al_2O_3$ ,  $BeO$  and  $MgO$ , follow this type of two-stage behavior as outlined by Davidge and Evans [22]. The classic model of Hall-Petch fracture is based on the same ideas of plastic deformation of grains and the pile-up of dislocations at grain boundaries outlined for Region II; however, the Petch model does not incorporate the concept of a pre-existing flaw or crack [24].

Given that dislocations are seldom observed in nanostructured ceramics [19] and the fact that dislocations in brittle ceramics are relatively immobile at low temperatures even when present [25], it would appear that the hardness improvement observed in our nano-TiN is not due to "Region II," or classical Hall-Petch, plastic deformation/dislocation fracture. Additionally, Averback *et al.*, while stating that the reasons for their observed Hall-Petch-like behavior in nano- $TiO_2$  are "presently unclear," do note

that dislocations are unlikely to be involved for grain sizes below 400 nm [21]. Thus, it seems most probable that the increased hardness for TiN with decreasing grain size, over the grain size range outlined above, is due to reductions in the inherent flaw sizes (Region I behavior) with reductions in the particle and grain sizes of our materials.

The fracture toughness values are comparable to those reported in other dense TiN materials. No dependence on, or benefit from, a nanostructure is expected for fracture toughness values. For instance, in fully dense  $\text{TiO}_2$ , when the grain size was less than 500 nm, the fracture toughness was independent of grain size and similar to that found in single crystal  $\text{TiO}_2$  [19]. Thus, it is not surprising that the  $K_c$  values reported here for our nanostructured TiN ( $4.0 \text{ MPa m}^{\frac{1}{2}}$ ) materials fall within the range of other values ( $3.5 - 4.3 \text{ MPa m}^{\frac{1}{2}}$  [12,26]) for TiN described in the literature.

### Summary

The processing scheme we have developed for our nano-TiN powders generated a dense, nanostructured TiN material, with final grain sizes of  $\sim 140$  nm, through a pressureless sintering process emphasizing improved powder handling procedures. These fine-grained materials have values of  $H_v$  (23.2 GPa) which are among the highest recorded in the literature for TiN. These sintering and property results are particularly noteworthy in comparison to those noted previously in the literature due to the complicated processing conditions required by other researchers utilizing lower quality starting powders.

### References

- [1] J.Y. Ying, ONR Technical Report, September 30, 1996.
- [2] D.T. Castro and J.Y. Ying, unpublished results, M.I.T.
- [3] G.R. Anstis, P. Chantikul, B.R. Lawn, and D.B. Marshall, "A Critical Evaluation of Indentation Techniques for Measuring Fracture Toughness: I, Direct Crack Measurements," *J. Am. Ceram. Soc.*, **64** [9] 533-538 (1981).
- [4] R.A. Andrievski, "Physical-Mechanical Properties of Nanostructured Titanium Nitride," *Nanostr. Mater.*, **9** 607-610 (1997).
- [5] R.A. Andrievski, "Particulate Nanostructured Silicon Nitride and Titanium Nitride," *ACS Symposium Series*, **622** 294-301 (1996).
- [6] B.O. Johansson, J.-E. Sundgren, J.E. Greene, A. Rockett, and S.A. Barnett, "Growth and Properties of Single Crystal TiN Films Deposited by Reactive Magnetron Sputtering," *J. Vac. Sci. Technol. A*, **3** [2] 303-307 (1985).
- [7] R. Naß, S. Albayrak, M. Aslan, and H. Schmidt, "Processing and Sintering of Nanosized TiN," pp. 47-54 in Advanced Materials in Optics, Electro-Optics and Communication Technologies, P. Vincenzini, ed., (Techna Srl, 1995).
- [8] R. Naß, S. Albayrak, M. Aslan, and H. Schmidt, "Colloidal Processing and Sintering of Nano-Scale TiN," *Ceram. Trans.*, **51** 591-596 (1995).
- [9] E. Rapoport, C. Brodhag, and F. Thévenot, "Hot Pressing of Titanium Nitride Powders," *Revue de Chimie minérale*, **22** [4] 456-466 (1985).
- [10] T. Yamada, M. Shimada, and M. Koizumi, "Fabrication and Characterization of Titanium Nitride by High Pressure Hot Pressing," *Am. Ceram. Soc. Bull.*, **59** [6] 611-616 (1981).
- [11] T. Yamada, M. Shimada, and M. Koizumi, "Fabrication and Characterization of Titanium Nitride by High Pressure Hot Pressing," *Ceram. Bull.*, **59** [6] 611-616 (1980).
- [12] S. Torizuka and T. Kishi, "Effect of SiC and  $\text{ZrO}_2$  on Sinterability and Mechanical Properties of Titanium Nitride, Titanium Carbonitride and Titanium Diboride," *Materials Transactions, JIM*, **37** [4] 782 - 787 (1996).
- [13] R.A. Andrievski, R.A. Lyutikov, O.D. Torbova, V.I. Torbov, V.G. Vil'chinskii, O.M. Grebtsova, E.P. Domashneva, A.A. Eremenko, and A.Z. Rakhmatullina, "Gas Evolution and Porosity Changes During Sintering of Highly Dispersed Titanium Nitride," *Inorg. Mater.*, **29** [12] 1474-1477 (1993).

[14] L. Cao, S.O. Yang, and Y. Tang, "Synthesis of Titanium Nitride Nanostructured Materials," *Trans. Mat. Res. Soc. Jpn.*, **16B** 1505-1508 (1994).

[15] M. Moriyama, K. Komata, and Y. Kobayashi, "Mechanical and Electrical Properties of Hot-Pressed TiN Ceramics Without Additives," *J. Ceram. Soc. Jpn.*, **99** 286-291 (1991).

[16] Y. Ogino, M. Miki, T. Yamasaki, and T. Inuma, "Preparation of Ultrafine-Grained TiN and (Ti,Al)N Powders by Mechanical Alloying," *Mater. Sci. Forum*, **88-90** 795-800 (1992).

[17] T. Rabe and R. Wäsche, "Development of Dense Nanocrystalline Titanium Nitride," *Ceram. Trans.*, **51** 793-798 (1995).

[18] K. A. Padmanabhan and H. Hahn, "Microstructures, Mechanical Properties and Possible Applications of Nanostructured Materials," pp. 21-32 in Synthesis and Processing of Nanocrystalline Powder, ed. D.L. Bourell, (The Minerals, Metals & Materials Society, 1996).

[19] H. Hahn and K.A. Padmanabhan, "Mechanical Response of Nanostructured Materials," *Nanostr. Mater.*, **6** 191-200 (1995).

[20] R.A. Andrievskii, "Synthesis and Properties of Nanocrystalline Refractory Compounds," *Russian Chem. Rev.*, **63** [5] 411-427 (1994).

[21] R.S. Averback, H.J. Höfler, H. Hahn, and J.C. Logas, "Sintering and Grain Growth in Nanocrystalline Ceramics," *NanoStr. Mater.*, **1** 173-178 (1992).

[22] R.W. Davidge and A.G. Evans, "The Strength of Ceramics," *Mater. Sci. Eng.*, **6** 281-298 (1970).

[23] S.C. Carniglia, "Reexamination of Experimental Strength-vs-Grain Size Data for Ceramics," *J. Am. Ceram. Soc.*, **55** [5] 243-249 (1972).

[24] N.J. Petch, "Cleavage Strength of Polycrystals," *J. Iron Steel Inst.*, **174** [1] 25-28 (1953).

[25] M.G.S. Naylor and T.F. Page, "Microstructural Studies of the Temperature-Dependence of Deformation Structures Around Hardness Indentations in Ceramics," *J. Microscopy*, **130** 345-360 (1983).

[26] V.F. Berdikov, Y.N. Vil'k, O.I. Pushkarev, and E.A. Lavrenova, "Micromechanical Characteristics of Hot-Pressed Titanium Nitride from Ultradispersed Powders," *Strength of Mater.*, **25** [3] 228-230 (1993).

TABLE 1: Comparison of Processing Routes and Properties of TiN

Researcher(s)	Technique/Conditions	Density	Grain Size (nm)	$H_v$ (GPa)
R.A. Andrievski [4]	Hot Press: 4 – 7.7 GPa, 1300 °C (16 – 18 nm)	95%	30 - 60	26.0 ± 1.0
R.A. Andrievski [4,5]	Hot Press: 4 GPa, 1200 °C (80 nm)	98%	100 - 200	23.5 ± 1.1
<b>Castro and Ying</b>	<b>Pressureless: 0.1 MPa N<sub>2</sub>, 1400 °C</b>	<b>99%</b>	<b>140</b>	<b>23.2 ± 1.9</b>
B.O. Johansson [6]	Magnetron Sputtering	100%	Single Crystal	22.6 ± 2.0
R. Naβ [7,8]	Pressureless: 1400 °C (colloidal processing)	98%	400	21.5
E. Rapoport [9]	Hot Press: 40 MPa, 1600 °C	97.5%	5,000 – 6,000	18.1
T. Yamada [10,11]	Hot Press: 40 MPa, 1600 °C	95% (of theo.)	1,450	18.0
S. Torizuka [12]	Pressureless (1700 °C) plus HIP (200 MPa, 1600 °C)	100%	20,000+	13.7
R.A. Andrievski [13]	Pressureless: 1500 °C (80 nm)	86%	500 - 5000	10 - 18
L. Cao [14]	Pressureless: 1300 °C (2.5 GPa initial compaction)	95%	180	12.8
M. Moriyama [15]	Hot Press: 140 MPa, 2100 °C	94%	10,000+	10 - 11
Y. Ogino [16]	Pressureless: 1300 °C (ball milled powders, 11.8 at% Fe/Cr)	99%	200	9.9
T. Rabe [17]	Gas Pressure Sintering: 5 MPa N <sub>2</sub> , 1300 °C	98%	100	-

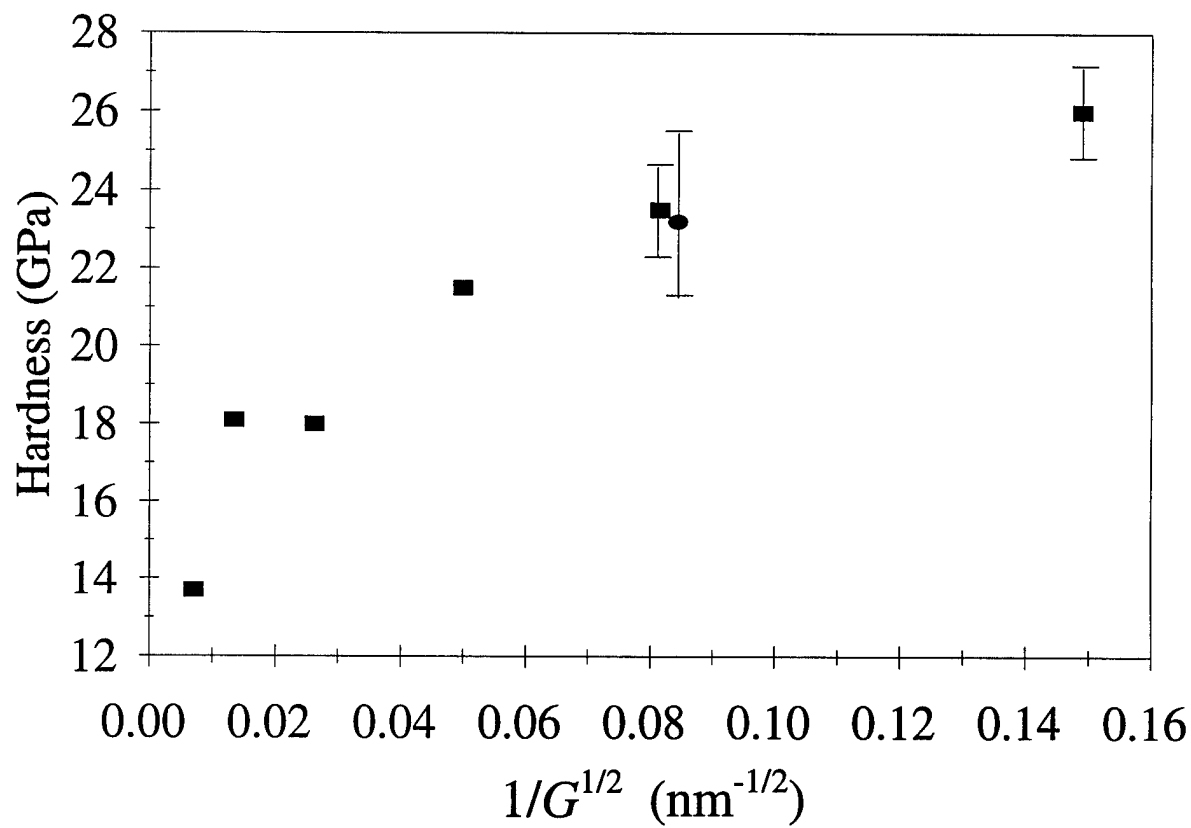


Figure 1: Hardness dependence on grain size for TiN.